Supersymmetry transformation for excitation processes

Jérôme Margueron* and Philippe Chomaz
GANIL, CEA/DSM-CNRS/IN2P3, Boîte Postale 5027, F-14076 Caen Cedex 5, France
(Received 2 February 2004; revised manuscript received 19 November 2004; published 28 February 2005)

Quantum mechanics super symmetry (SuSy) provides a general framework for studies using phenomenological potentials for nucleons (or clusters) interacting with a core. The SuSy potentials result from the transformation of the mean-field potential to account for the Pauli blocking of the core orbitals. In this article, we discuss how other potentials (such as external probes or residual interactions between the valence nucleons) are affected by the SuSy transformation. We illustrate how the SuSy transformations induce off-diagonal terms in coordinate space that play an essential role on the induced transition probabilities for two examples: electric operators and Gaussian external fields. We show that excitation operators, doorway states, strength, and sum rules are all modified.

DOI: 10.1103/PhysRevC.71.024318 PACS number(s): 21.60.−n, 11.30.Pb, 21.10.Pc, 24.10.−i

I. INTRODUCTION

Almost all branches of many-body physics have developed methods to simplify a many-body self-interacting system into a local "effective" mean potential affecting the pertinent degrees of freedom. This simplification often provides an adequate starting point for more sophisticated approaches. For example, phenomenological potentials replacing the Schrödinger equation of N self-interacting particles by a one-body potential whose orbits simulate an experimentally known structure have been widely used in nuclear physics. Of particular interest are the halo systems, which are often described in terms of valence nucleons interacting with a core. An elegant way to justify the effective core-nucleon phenomenological interaction is to invoke a supersymmetric (SuSy) transformation of the mean-field potential of an N-body system [1–5]. Indeed, since the core is made of nucleons occupying the lowest orbitals of the mean-field potential, the halo nucleons cannot fill in these occupied states because of the Pauli exclusion principle. SuSy transformations including the forbidden states removal (states removal potential, SRP) and the restoration of phase shifts (phase equivalent potential, PEP) provide an exact way to remove the states occupied by the core without altering the remaining states' properties. Hence, SuSy transformation, which can be fully analytical for some classes of potentials [5], provides an equivalent effective interaction between composite systems and thus can be safely used to describe nuclear structure and reaction of nuclei presenting a high degree of clusterization.

SuSy transformations have been applied to breakup mechanisms involving halo nuclei [6,7]. Indeed, the phenomenological treatment of halo nuclei in terms of nucleons interacting with a core should take into account the fact that some intrinsic bound states of the nucleon-core potential are Pauli blocked. For instance, the 1s orbital is generally occupied by the core nucleons. In the case of a one-neutron halo, such as for ^{11}Be or ^{19}C, SuSy-PEP potentials have been used to calculate $B(E1)$ matrix elements [6], Coulomb breakup [7], and transfer reactions [8]. In the case of a two-neutron halo, such as for ^{6}He, ^{11}Li, or ^{14}Be, SuSy transformations have been applied to remove the forbidden states and to analyze binding energies and radii of these nuclei [9–12]. Finally, SuSy transformations have also been included in coupled-channel calculations [13–15]. In all these calculations, the SuSy transformation has been applied under the following approximation: Only the internal part of the Hamiltonian (the core-halo potential) is SuSy transformed whereas the additional fields (external potentials and two-body correlations in the halo) remain unmodified. This approximation will be called the *internal* SuSy approximation because it concerns only the core-halo potential. In the framework of this approximation, the SuSy transformation is not equivalent to the exact treatment in which the Pauli-blocked states are projected out. In this article, we discuss a consistent SuSy framework that is always equivalent to the full projection method.

The accuracy of the *internal* SuSy transformation has been discussed in several papers. For instance, Ridikas *et al*. [6] have analyzed the radii of several halo nuclei as well as $B(E1)$ matrix elements before and after the SuSy transformation. Thompson *et al*. [10] and Descouvemont *et al*. [12] have performed a comparison of the full projector method with the *internal* SuSy. Because the consistent SuSy framework we discuss is totally equivalent to the full projection method, the comparison between the *internal* approximation and the consistent SuSy treatment is thus an alternative method for estimating the accuracy of the *internal* approximation. From the theoretical point of view, the consistent SuSy approach provides a unique and exact framework to compute excitation processes or to take into account residual interaction between valence nuclei. Such a consistent framework is essential interpret the results of inverse problems in scattering theory [16].

This article is organized in the following way. In Sec. II, we develop a consistent formalism to map the original Hamiltonian into the SuSy partner Hamiltonian. In the case of a static problem, this mapping is the usual one, but we will show in Sec. III that in the case of a Hamiltonian modified by either an external field or a two-body interaction (for instance, two neutrons in the halo), one should transform these fields into the new space. In Sec. IV, we will illustrate the SuSy transformation, showing both analytical results and numerical implementations for two potentials that are important in

*Present address: Institute für Theoretische Physik, Universität Tübingen, D-72076 Tübingen, Germany.

nuclear physics. We will then discuss the transformation of an external field: the response to an electric excitation of the general form $\hat{r}^\lambda \hat{Y}_{LM}$ in Sec. V, and the response to a Gaussian potential in Sec. VI.

II. SUSY TRANSFORMATION FOR THE ONE-BODY HAMILTONIAN

The application of supersymmetry to Schrödinger quantum mechanics [1–5] has shed new light on the problem of constructing phase-equivalent potentials. In this section, we review the SuSy transformations that remove a state (SRP) and impose that the phase shifts are conserved (PEP) [17,18]. We will introduce mapping operators that change the Hamiltonian as well as the bound states. Finally we will present effects on the external potential and residual interaction of composite systems described through effective Hamiltonians.

A. Initial Hamiltonian: $\hat{h}_0$

Quantum mechanics SuSy has been extensively studied for one-dimensional systems. There are two ways to perform the multidimensional generalization depending on the choice of space coordinates. In three dimensions, one can choose Cartesian coordinates (x, y, z) [2] or spherical coordinates (r, Ω) [3]. We choose the latter, which is often used for excitation processes. Hence, the representation of the one-particle Hilbert space $\mathcal{H}$ is given by a sum over the subspaces $\mathcal{H}^l$ associated with the angular momentum l: $\mathcal{H} = \mathcal{H}^0 + \mathcal{H}^1 + \mathcal{H}^2 + \cdots$.

Let us introduce the initial Hamiltonian

$$\hat{h}_0 = \frac{\hat{\mathbf{p}}^2}{2m} + \hat{\mathrm{v}}_0, \tag{1}$$

where $\hat{\mathbf{p}}$ is the momentum operator and the potential operator $\hat{\mathrm{v}}_0$ is assumed to be local. Since $\hat{h}_0$ is rotationally invariant we can introduce angular momentum as a good quantum number and thus the wave functions associated with an energy E can be written as $|\phi_0(E)\rangle = \frac{1}{\hat{r}}|\varphi_0^l(E)\rangle \otimes |Y_{lm}\rangle$. In the subspace $\mathcal{H}^l$, the radial, static Schrödinger equation associated with the lth partial wave is

$$\hat{h}_0^l \left|\varphi_0^l(E)\right\rangle \equiv \left(\frac{\hat{p}^2}{2m} + \hat{v}_0^l\right)\left|\varphi_0^l(E)\right\rangle = E\left|\varphi_0^l(E)\right\rangle, \tag{2}$$

where $\hat{p} = i\hbar\,\hat{\nabla}_r$ is the radial momentum operator. The effective radial potential $\hat{v}_0^l$ includes the centrifugal force

$$\hat{v}_0^l = \frac{\hbar^2}{2m}\frac{l(l+1)}{\hat{r}^2} + \hat{\mathrm{v}}_0. \tag{3}$$

To simplify the discussion, we do not include the spin-orbit potential. Nevertheless, the generalization of this framework to include spin-orbit potential is not difficult.

To simplify the notation, when there is no ambiguity we will drop the label l since the SuSy transformations considered are defined in a subspace of angular momentum l (and m) (i.e., they are block-diagonal in the complete space. Thus, they affect differently the potential $\hat{v}^l$ associated with different l.

B. Hamiltonian after k SuSy transformations: $\hat{h}_k$

The elementary SuSy transformations remove a single state with or without restoring the phase shifts. To remove several states we will iterate the SuSy transformation. Therefore, let us assume that after k transformations the radial, static Schrödinger equation associated with the lth partial wave can be written as

$$\hat{h}_k^l \left|\varphi_k^l(E)\right\rangle \equiv \left(\frac{\hat{p}^2}{2m} + \hat{v}_k^l\right)\left|\varphi_k^l(E)\right\rangle = E\left|\varphi_k^l(E)\right\rangle. \tag{4}$$

It should be noticed that, since the SuSy transformations are block diagonal and different in each subspace of angular momentum l, the different radial potentials do not correspond to the same potential; that is, the various $\hat{\mathrm{v}}_k^l$,

$$\hat{\mathrm{v}}_k^l = \hat{v}_k^l - \frac{\hbar^2}{2m}\frac{l(l+1)}{\hat{r}^2}, \tag{5}$$

are different for different angular momenta l. We call $E_k^{(i)}$ $(i = n, l)$ the energy of the ith bound state of $\hat{h}_k^l$, which is thus $(2l+1)$-fold degenerate.

The bound states correspond to the square integrable solutions of the differential equation (4). However, we will not restrict the solution of Eq. (4) to bound states but rather consider all solutions $|\varphi_k(E)\rangle$. Given a particular solution $|\widetilde{\varphi}_k(E)\rangle$ of Eq. (4) whose inverse is square integrable, the general solution of Eq. (4) can be recast as [3]

$$\varphi_k(E, \alpha; r) = \widetilde{\varphi}_k(E; r)\left(1 + \alpha\int_r^\infty \frac{dr'}{[\widetilde{\varphi}_k(E; r')]^2}\right), \tag{6}$$

where the parameter α can vary freely to construct all the possible solutions of the second-order differential equation (4), up to a multiplicative factor and provided that $\alpha = \infty$ is allowed. In Eq. (6), we use the r representation and the Dirac notation: $\widetilde{\varphi}_k(E; r) = \langle r\,|\widetilde{\varphi}_k(E)\rangle$. For future use let us define the constant $\beta = [\int_0^\infty dr/(\widetilde{\varphi}_k(E; r))^2]^{-1}$.

The Hamiltonians $\hat{h}_k$ can always be factorized as

$$\hat{h}_k = \hat{a}_k^+\hat{a}_k^- + \mathcal{E}_k, \tag{7}$$

where $\mathcal{E}_k$ is the factorization energy and the first-order differential operators $\hat{a}_k^\pm$ $[\hat{a}_k^- = (\hat{a}_k^+)^\dagger]$ are of the following form:

$$\hat{a}_k^\pm = \frac{1}{\sqrt{2m}}(\hbar\hat{w}_k \mp i\,\hat{p}), \tag{8}$$

where $\hat{w}_k \equiv w_k(\hat{r})$ is the superpotential. Notice that, in the literature, capital letters are usually used for the differential operators $\hat{a}_k^\pm$. Here, we dedicate capital letters for many-body operators and use lowercase letters for the one-body operator. It is possible to show that the general solution $|\varphi_k(\mathcal{E}_k, \alpha)\rangle$ of Eq. (4) with $E = \mathcal{E}_k$ is equivalently the solution of the first-order differential equation

$$\hat{a}_k^-\,|\varphi_k(E = \mathcal{E}_k, \alpha)\rangle = 0. \tag{9}$$

As a consequence, the superpotential is the local operator defined by

$$w_k(E = \mathcal{E}_k, \alpha; r) = \frac{d}{dr}\ln\varphi_k(E = \mathcal{E}_k, \alpha; r). \tag{10}$$

For a given factorization energy $\mathcal{E}_k$, there is a family of solutions that depends on the parameter α generating the superpotential $\hat{w}_k(E=\mathcal{E}_k,\alpha)$. Note that $\varphi_k(E=\mathcal{E}_k,\alpha;r)$ must be nodeless for $\hat{a}_k^{\pm}$ to be bound. Hence $\mathcal{E}_k$ must be less than or equal to the ground-state energy E_k of $\hat{h}_k$ and this requires also that $\alpha > -\beta$. The choice of the factorization energy $\mathcal{E}_k$ and the selection of a member from the family of solutions w_k must clearly be physically motivated.

In this section we have defined the notation used in the following. In the next section we will present a two-step method that removes the lowest energy state and preserves the phase shifts.

C. State removal potential: $\hat{v}_{k+1}$

The SRP transformation is defined so that it removes the lowest energy state of a given subspace $\mathcal{H}^l$. For the given angular momentum l, we choose $\mathcal{E}_k = E_k^0$, the energy of the lowest energy state of the Hamiltonian $\hat{h}_k$. It follows that the inverse of the particular solution $|\tilde{\varphi}_k(E)\rangle$ is not square integrable, which imposes $\alpha = 0$. With these definitions, we associate with $\hat{h}_k$ a supersymmetric partner $\hat{h}_{k+1}$ defined by

$$\hat{h}_{k+1} = \hat{a}_k^- \hat{a}_k^+ + \mathcal{E}_k = \frac{\hat{p}^2}{2m} + \hat{v}_{k+1}, \tag{11}$$

$$\hat{v}_{k+1} = \hat{v}_k - \frac{\hbar^2}{m}(\partial_r\ \hat{w}_k(\mathcal{E}_k, \alpha = 0)). \tag{12}$$

The Hamiltonians $\hat{h}_k$ and $\hat{h}_{k+1}$ share the same spectrum except for the lowest energy state of $\hat{h}_k$, which has been suppressed in $\hat{h}_{k+1}$. The states $[|\varphi_{k+1}(E)\rangle]$ of $\hat{h}_{k+1}$ can be obtained from those $[|\varphi_k(E)\rangle]$ of $\hat{h}_k$ according to

$$|\varphi_{k+1}(E)\rangle = \frac{1}{\sqrt{\hat{h}_{k+1} - \mathcal{E}_k}} \hat{a}_k^- |\varphi_k(E)\rangle \equiv \hat{\mathrm{u}}_k^- |\varphi_k(E)\rangle . \tag{13}$$

Conversely, except for the ground state, the states of $\hat{h}_k$ can be obtained from those of $\hat{h}_{k+1}$ by

$$|\varphi_k(E)\rangle = \frac{1}{\sqrt{\hat{h}_k - \mathcal{E}_k}} \hat{a}_k^+ |\phi_{k+1}(E)\rangle = \hat{\mathrm{u}}_k^+ |\varphi_{k+1}(E)\rangle.$$

In these equations, we have introduced the pseudo-unitary SRP operators $\hat{\mathrm{u}}_k^-$ and $\hat{\mathrm{u}}_k^+$, which are defined as (the products $\hat{a}_k^+\hat{a}_k^-$ and $\hat{a}_k^-\hat{a}_k^+$ being definite positive)

$$\hat{\mathrm{u}}_k^+ = \hat{a}_k^+ \frac{1}{\sqrt{\hat{a}_k^-\hat{a}_k^+}} = \frac{1}{\sqrt{\hat{a}_k^+\hat{a}_k^-}} \hat{a}_k^+, \tag{14}$$

$$\hat{\mathrm{u}}_k^- = \hat{a}_k^- \frac{1}{\sqrt{\hat{a}_k^+\hat{a}_k^-}} = \frac{1}{\sqrt{\hat{a}_k^-\hat{a}_k^+}} \hat{a}_k^-. \tag{15}$$

These operators are pseudo-unitary since $\hat{\mathrm{u}}_k^- = (\hat{\mathrm{u}}_k^+)^\dagger$, $\hat{\mathrm{u}}_k^-\hat{\mathrm{u}}_k^+ = \hat{1}$, and $\hat{\mathrm{u}}_k^+\hat{\mathrm{u}}_k^- = \hat{\mathrm{p}}$, where the projector $\hat{\mathrm{p}}$ suppresses the lowest energy state $|\varphi_k^0\rangle$ of the Hamiltonian $\hat{h}_k$ from the subspace $\mathcal{H}^l$ and can be written as $\hat{\mathrm{p}} = 1 - |\varphi_k^0\rangle\langle\varphi_k^0|$.

The relation between $\hat{h}_k$ and $\hat{h}_{k+1}$ is

$$\hat{h}_{k+1} = \frac{\hat{p}^2}{2m} + \hat{v}_{k+1} = \hat{\mathrm{u}}_k^- \left(\frac{\hat{p}^2}{2m} + \hat{v}_k\right) \hat{\mathrm{u}}_k^+ = \hat{\mathrm{u}}_k^-\ \hat{h}_k\ \hat{\mathrm{u}}_k^+. \tag{16}$$

However, it is important to remark that $\hat{v}_{k+1} \neq \hat{\mathrm{u}}_k^-\hat{v}_k\hat{\mathrm{u}}_k^+$ and $\hat{p}^2 \neq \hat{\mathrm{u}}_k^-\hat{p}^2\hat{\mathrm{u}}_k^+$. In fact the SuSy transformation of a local potential is not local. The simple diagonal form of the potential given by Eq. (12) is recovered because, by construction, the modifications of the kinetic part just cancel the off-diagonal terms in the transformed potential. Then, the kinetic and the potential parts of the Hamiltonian should be transformed together to get the relation (16) with simple potential (local in r space) and kinetic (diagonal in the p representation) terms.

D. Phase equivalent potential: $\hat{v}_{k+1}$

It can be shown that SRP transformations change the phase shifts. To solve this problem, Baye [4] has proposed performing a second SuSy transformation and associating to $\hat{h}_{k+1}$ a new supersymmetric partner $\underline{\hat{h}}_{k+1}$ so that

$$\underline{\hat{h}}_{k+1} = \underline{\hat{a}}_k^-\underline{\hat{a}}_k^+ + \underline{\mathcal{E}}_k = \frac{\hat{p}^2}{2m} + \underline{\hat{v}}_{k+1}, \tag{17}$$

with $\underline{\mathcal{E}}_k = E_k^0$, the ground-state energy of $\hat{h}_k$, and $\alpha = -\beta$. In this case, the solution $\underline{\varphi}_{k+1}$ of $\underline{\hat{h}}_{k+1}$ and its inverse are not square integrable. The spectra of $\hat{h}_{k+1}$ and $\underline{\hat{h}}_{k+1}$ are strictly identical; the second SuSy transformation does not suppress nor add any state, but it restores the phase shifts so that the Hamiltonian $\underline{\hat{h}}_{k+1}$ is equivalent to $\hat{h}_k$ as far as the scattering properties are concerned. Note that the energy $\underline{\mathcal{E}}_k = E_k^0$ is now below the ground-state energy E_{k+1}^0 of $\hat{h}_{k+1}$.

The corresponding superpotential $\underline{\hat{w}}_k(\underline{\mathcal{E}}_k)$ is deduced from the wave function $|\varphi_{k+1}(\mathcal{E}_k = E_k^0)\rangle$ of $\hat{h}_{k+1}$ within the following relation:

$$\underline{w}_k(\mathcal{E}_k,\alpha;r) = \frac{d}{dr}\ln\varphi_{k+1}(E=\mathcal{E}_k,\alpha;r), \tag{18}$$

which is equivalent to Eq. (10). It can also be deduced directly from the ground state of $\hat{h}_k$ according to [17]:

$$\begin{aligned}\underline{w}_k(\underline{\mathcal{E}}_k;r) &= \frac{d}{dr}\ln\frac{1}{\varphi_k^0(r)}\int_0^r dr'\ \left(\varphi_k^0(r')\right)^2 \\ &= \underline{\underline{w}}_k(\mathcal{E}_k;r) - w_k(\mathcal{E}_k;r),\end{aligned} \tag{19}$$

where we have used the relation $\underline{\mathcal{E}}_k = \mathcal{E}_k$ and introduced the modified superpotential $\underline{\underline{w}}_k(\mathcal{E}_k;r)$ as

$$\underline{\underline{w}}_k(\mathcal{E}_k;r) = \frac{d}{dr}\ln\int_0^r dr'\ \left(\varphi_k^0(r')\right)^2. \tag{20}$$

The corresponding potential $\underline{\hat{v}}_{k+1}$ is

$$\begin{aligned}\underline{\hat{v}}_{k+1} &= \hat{v}_{k+1} - \frac{\hbar^2}{m}(\partial_r\ \underline{\hat{w}}_k(\mathcal{E}_k)) \\ &= \hat{v}_k - \frac{\hbar^2}{m}(\partial_r\ \underline{\underline{\hat{w}}}_k(\mathcal{E}_k)).\end{aligned} \tag{21}$$

According to this discussion, the spectra of $\hat{h}_{k+1}$ and $\underline{\hat{h}}_{k+1}$ are identical. All the states of $\hat{h}_k$, except its lowest energy state, are mapped onto the states of $\underline{\hat{h}}_{k+1}$ and those two Hamiltonians have the same phase shifts. This mapping is simply

$$|\underline{\varphi}_{k+1}(E)\rangle = \frac{1}{E_k^0 - \underline{\hat{h}}_{k+1}}\underline{\hat{a}}_k^-\hat{a}_k^-\ |\varphi_k(E)\rangle \equiv \underline{\hat{\mathrm{u}}}_k^-\ \left|\varphi_k^l(E)\right\rangle, \tag{22}$$

$$|\varphi_k(E)\rangle = \frac{1}{E_k^0 - \hat{h}_k}\hat{a}_k^+\underline{\hat{a}}_k^+|\underline{\varphi}_{k+1}(E)\rangle = \underline{\hat{u}}_k^+|\underline{\varphi}_{k+1}(E)\rangle, \quad (23)$$

with the pseudo-unitary PEP operators

$$\underline{\hat{u}}_k^+ = -\hat{a}_k^+\underline{\hat{a}}_k^+\frac{1}{\hat{a}_k^-\underline{\hat{a}}_k^+} = -\frac{1}{\hat{a}_k^+\hat{a}_k^-}\hat{a}_k^+\underline{\hat{a}}_k^+, \quad (24)$$

$$\underline{\hat{u}}_k^- = -\frac{1}{\underline{\hat{a}}_k^-\underline{\hat{a}}_k^+}\underline{\hat{a}}_k^-\hat{a}_k^- = -\underline{\hat{a}}_k^-\hat{a}_k^-\frac{1}{\hat{a}_k^-\hat{a}_k^+}, \quad (25)$$

The relation between $\hat{h}_k$ and $\underline{\hat{h}}_{k+1}$ is

$$\underline{\hat{h}}_{k+1} = \underline{\hat{u}}_k^-\,\hat{h}_k\,\underline{\hat{u}}_k^+. \quad (26)$$

The advantage of using the operators $\hat{u}_k^\pm$ and $\underline{\hat{u}}_k^\pm$ is that all the relations we will deduce hereafter will be algebraically equivalent for SRP and PEP transformations. In the following, as long as no confusion is possible, we will write the relations fulfilled by the general operator $\hat{u}_k^\pm$, which can be replaced by either the operator $\hat{u}_k^\pm$ for the SRP transformation or $\underline{\hat{u}}_k^\pm$ for the PEP one.

III. SUSY TRANSFORMATION FOR GENERAL HAMILTONIANS

In nuclear physics, we are often interested in the description of A interacting nucleons assuming that these nucleons can be separated into a frozen core containing A_c nucleons and a valence space containing A_v nucleons. Hence, the wave function of this system is assumed to factorize into a core and a valence part, $|\Phi(A_c + A_v)\rangle = |\Phi_c(A_c)\rangle \otimes |\Phi_v(A_v)\rangle$. The core state is described at the mean-field level as a Slater determinant, $|\Phi_c(A_c)\rangle$, of A_c single-particle states $|\phi_h\rangle$ occupying the $h = 1, A_c$ lowest energy eigenstates of the mean-field potential $\hat{h}_0$: $|\Phi_c(A_c)\rangle = \widetilde{\prod}_{h=1}^{A_c}|\phi_h\rangle$, where $\widetilde{\prod}$ stands for the antisymmetrization sign. As a consequence of the Pauli principle, the valence nucleons cannot occupy the lowest orbitals of the core-valence potential, which are already occupied by the core nucleons. The evolution of $|\Phi_v(A_v)\rangle$ is thus ruled by the Hamiltonian $\hat{H}_v$, which contains a projection out of the occupied space $\hat{P}_v = \prod_{h=1}^{A_c}\hat{c}_h\hat{c}_h^+$, where $\hat{c}_h^+$ ($\hat{c}_h$) is the creation (annihilation) operator of a nucleon in the occupied orbital $|\phi_h\rangle$. $\hat{H}_v$ is assumed to contain the confining effect of the mean field $\hat{h}_0$. For cases with several nucleons in the valence space, the residual interaction among valence nucleons, $\hat{V}_0$, should be taken into account when the problem of correlations is addressed. Finally, an external field, $\hat{f}_0$, should be introduced to compute excitation properties. Then the Hamiltonian reads

$$\hat{H}_v = \hat{P}_v\hat{H}\hat{P}_v \quad (27)$$

with

$$\hat{H} = \sum_{i=1}^{A_v}\hat{h}_0(i) + \frac{1}{2}\sum_{i,j=1}^{A_v}\hat{V}_0(i,j) + \sum_{i=1}^{A_v}\hat{f}_0(i). \quad (28)$$

In the following, we propose to generalize the SuSy transformation so that it remains totally equivalent to the projector method for every kind of additional potential.

The first step of this method is to remove, from the single-particle states accessible to a valence nucleon i, the A_c orbitals occupied by the core nucleons. To perform this, for each particle i of the valence state, we introduce the full operator $\hat{U}_{A_c}^-(i)$, which is the product of A_c different SuSy transformations $\hat{u}_h^-(i)$ removing the occupied core states h [cf. Eqs. (14) and (24)],

$$\hat{U}_{A_c}^-(i) = \hat{u}_{h_{A_c}}^-(i)\,\hat{u}_{h_{A_c-1}}^-(i)\,...\,\hat{u}_{h_2}^-(i)\,\hat{u}_{h_1}^-(i). \quad (29)$$

In this equation, the operator $\hat{u}_h^-$ removing the occupied state $h = (n, l, m)$ with a principal quantum number n, orbital angular momentum l, and projection m (recalling that for simplicity we have not introduced the isospin and spin quantum numbers because these extensions are straightforward) affects only the (l, m) subspace. In the (l, m) subspace the operator is nothing but the $(n-1)$ SuSy transformation $\hat{u}_{n-1}^{l-}$ associated with the Hamiltonian $\hat{h}_0^l$ and it is the identity in all the other subspaces. The conjugated operator $\hat{U}_{A_c}^+(i)$ reads

$$\hat{U}_{A_c}^+(i) = \hat{u}_{h_1}^+(i)\hat{u}_{h_2}^+(i)...\,\hat{u}_{h_{A_c-1}}^+(i)\,\hat{u}_{h_{A_c}}^+(i). \quad (30)$$

Since those different transformations affect only a given single-particle (l, m) subspace, the total operator $\hat{U}_{A_c}^\pm(i)$ is block diagonal in spin representation. Being the product of pseudo-unitary transformations, $\hat{U}_{A_c}^\pm(i)$ is also pseudo-unitary since $\hat{U}_{A_c}^-(i) = (\hat{U}_{A_c}^+(i))^\dagger$, $\hat{U}_{A_c}^-(i)\hat{U}_{A_c}^+(i) = \hat{1}(i)$, and $\hat{U}_{A_c}^+(i)\hat{U}_{A_c}^-(i) = \hat{P}_v(i)$, where $\hat{1}(i)$ and $\hat{P}_v(i)$ are respectively, the identity $\hat{1}$ and projection operator $\hat{P}_v$ restricted to the single-particle space of the particle i.

The second step is to apply the complete SuSy transformation $\hat{U}_{A_c}^\pm(i)$ on each valence nucleon i,

$$\hat{U}_{A_c}^\pm = \prod_{i=1}^{A_v}\hat{U}_{A_c}^\pm(i). \quad (31)$$

Because $\hat{U}_{A_c}^\pm$ is a simple repetition on each single-particle space of the same operator pseudo-unitary transformations $\hat{U}_{A_c}^\pm(i)$, it is also a pseudo-unitary transformation, so $\hat{U}_{A_c}^- = (\hat{U}_{A_c}^+)^\dagger$, $\hat{U}_{A_c}^-\hat{U}_{A_c}^+ = \hat{1}$, and $\hat{U}_{A_c}^+\hat{U}_{A_c}^- = \hat{P}_v$, where $\hat{1}$ and $\hat{P}_v$ are, respectively, the identity and projection operators in the A_v-body Hilbert space associated with the A_v valence particles.

Using $\hat{U}_{A_c}^+\hat{U}_{A_c}^- = \hat{P}_v$, we can thus write $\hat{H}_v = \hat{P}_v\hat{H}\hat{P}_v$ and explicitly

$$\hat{H}_v = \hat{U}_{A_c}^+\hat{U}_{A_c}^-\hat{H}\hat{U}_{A_c}^+\hat{U}_{A_c}^- = \hat{U}_{A_c}^+\hat{H}_{v,A_c}\hat{U}_{A_c}^-, \quad (32)$$

where we have introduced the transformed Hamiltonian

$$\hat{H}_{v,A_c} = \hat{U}_{A_c}^-\hat{H}\hat{U}_{A_c}^+ = \sum_{i=1}^{A_v}\hat{h}_{A_c}(i) + \frac{1}{2}\sum_{i,j=1}^{A_v}\hat{V}_{A_c}(i,j) + \sum_{i=1}^{A_v}\hat{f}_{A_c}(i). \quad (33)$$

It is clear from this relation not only that $\hat{h}_0$ is transformed but also that the two-body interaction is changed into $\hat{V}_{A_c}(i, j)$. Using Eq. (31) and $\hat{U}_{A_c}^-(i)\,\hat{U}_{A_c}^+(i) = \hat{1}(i)$ we get

$$\hat{V}_{A_c}(i,j) = \hat{U}_{A_c}^-\hat{V}_0(i,j)\hat{U}_{A_c}^+ \quad (34)$$

$$= \hat{U}_{A_c}^-(i)\hat{U}_{A_c}^-(j)\hat{V}_0(i,j)\hat{U}_{A_c}^+(i)\hat{U}_{A_c}^+(j) \quad (35)$$

and the external potential $\hat{f}_0$ is mapped into

$$\hat{f}_{\mathrm{A_c}}(i) = \hat{\mathrm{U}}^{-}_{\mathrm{A_c}}\,\hat{f}_0(i)\hat{\mathrm{U}}^{+}_{\mathrm{A_c}} = \hat{\mathrm{U}}^{-}_{\mathrm{A_c}}(i)\,\hat{f}_0(i)\hat{\mathrm{U}}^{+}_{\mathrm{A_c}}(i). \tag{36}$$

Because $\hat{f}_{\mathrm{A_c}}(i)$ can induce transitions between two different angular momentum spaces, the mapping operators $\hat{\mathrm{u}}^{l^{\pm}}_{n}(i)$, which are important in $\hat{\mathrm{U}}^{\pm}_{\mathrm{A_c}}(i)$ on the right and on the left of Eq. (36), may not correspond to the same angular momentum l.

It should also be noticed that not only is the Hamiltonian changed but also the wave functions since the state of the valence nucleons is transformed into

$$\left|\Phi_{\mathrm{v,A_c}}(t)\right\rangle = \hat{\mathrm{U}}^{-}_{\mathrm{A_c}}\left|\Phi_{\mathrm{v}}(t)\right\rangle. \tag{37}$$

The evolution of a state $|\Phi_{\mathrm{v}}(t)\rangle$ is driven by the time-dependent Schrödinger equation

$$i\hbar\frac{d}{dt}\left|\Phi_{\mathrm{v}}(t)\right\rangle = \hat{H}_{\mathrm{v}}\left|\Phi_{\mathrm{v}}(t)\right\rangle, \tag{38}$$

which can be mapped into the new Hilbert space where the Pauli-blocked states have been removed within SuSy transformations:

$$i\hbar\frac{d}{dt}\left|\Phi_{\mathrm{v,A_c}}(t)\right\rangle = \hat{H}_{\mathrm{v,A_c}}\left|\Phi_{\mathrm{v,A_c}}(t)\right\rangle. \tag{39}$$

It is important to remark that the projectors $\hat{P}_{\mathrm{v}}$ involved in the definition of the valence Hamiltonian [cf. Eq. (27)] have been removed in the mapped Hamiltonian $\hat{H}_{\mathrm{v,A_c}}$ [cf. Eq. (33)]. Hence, the time-dependent Schrödinger equation in the SuSy space is simpler than the original Schrödinger equation, which involves projection operators. Nevertheless, the two Schrödinger equations written in the original space or in the SuSy-transformed Hilbert space contain strictly the same physical ingredients and are mathematically equivalent.

In the literature, the transformations of both the excitation operators and the wave functions are usually neglected (i.e., $\hat{f}_0$ is often used instead of $\hat{f}_{\mathrm{A_c}}$ and the wave functions are not transformed back when evaluating observables [6–11,13–15]). In the following, we will study a particularly important application: the evaluation of the response of the nucleus to an external (one-body) perturbation (time dependent or not). The use of a SuSy-transformed two-body residual interaction in the calculation of correlations and reactions will be the subject of forthcoming studies.

IV. EXAMPLES OF SUSY TRANSFORMATIONS

In this section, we illustrate the formalism just developed with two important physical examples: (i) the harmonic oscillator potential, which is mostly analytical and allows a deeper insight into the formalism while providing numerical tests, and (ii) the halo nuclei potential, which is of important physical interest but can be treated only numerically since only asymptotic relations can be deduced analytically.

A. The harmonic oscillator potential

The harmonic oscillator potential is a textbook example [19]. We set the local potential to be $V_0(r) = -V_0 + \frac{\hbar^2}{2m}(r/b)^2$ with $b^2 = \hbar/m\omega$. In the following, we introduce a reduced coordinate $x = r/b$.

The eigenstates are labeled with the quantum numbers (n, l, m) and are associated with a set of energies $E_{nl} = -V_0 + (2n + l + 3/2)\hbar\omega$. For each l the lowest energy state is

$$\varphi^{0l}_0(x) = c_l\, x^{l+1}\,\exp\left(-\tfrac{1}{2}x^2\right), \tag{40}$$

with $c_l = b^{l-1/2}/\pi^{3/4}$.

We deduce the following super potentials for SRP and PEP transformations:

$$w^l_0(x) = \frac{1}{b}\left(\frac{l+1}{x} - x\right), \tag{41}$$

$$\underline{\underline{w}}^l_0(x) = \frac{1}{b}\frac{x^{2l+2}\,e^{-x^2}}{\mathrm{erf}(x, 2l+2)}, \tag{42}$$

with the un-normalized error function defined by $\mathrm{erf}(z, l) = \int_0^z t^l e^{-t^2} dt$. The differential operators $\hat{a}^{l^{\pm}}_0$ are

$$\langle r|\hat{a}^{l^{\pm}}_0|r'\rangle = -\langle r|\frac{1}{\sqrt{2}}\left(\hat{x} \pm i\hat{q} - \hbar\omega\frac{l+1}{\hat{x}}\right)|r'\rangle, \tag{43}$$

$$\langle r|\underline{\hat{a}}^{l^{\pm}}_0|r'\rangle \underset{r,r'\to\infty}{\sim} -\langle r|\frac{1}{\sqrt{2}}\left(-\hat{x} \pm i\hat{q}\right)|r'\rangle, \tag{44}$$

where $\hat{x} = \sqrt{m\omega}\hat{r}$ and $\hat{q} = \hat{p}/\sqrt{m}$. Note that the PEP transformation could be confusing in this case because there are no phase for the harmonic oscillator potential. This transformation conserves the asymptotic normalization constants of the excited states, instead of the phase shifts, which are not defined in this case. Nevertheless, it remains interesting for discussion purposes.

From the expressions of the superpotentials removing only one state, we deduce the transformed potentials

$$v^l_1(r) = v^l_0(r) + \hbar\omega + \frac{\hbar^2(l+1)}{mr^2} = v^{l+1}_0(r) + \hbar\omega, \tag{45}$$

$$\underline{v}^l_1(r) = v^l_0(r) + \frac{\hbar^2}{mb^2}\frac{x^{2l+1}e^{-x^2}}{(\mathrm{erf}(x, 2l+2))^2} \times\left((2l + 2 - 2x^2)\mathrm{erf}(x, 2l+2) + x^{2l+3}\right). \tag{46}$$

These potentials are represented in Fig. 1. In the graphical illustrations we will use nuclear physics scales by taking the following parameters: $V_0 = 50$ MeV and $\hbar\omega = 10$ MeV. The lowest energy state is at -35 MeV. The right-hand side of Eq. (45) demonstrates that the SRP transformations removing only one state have mapped the original potential v^l_0 into a new potential, which is simply $v^{l'}_0 + \hbar\omega$, where the effective angular momentum is $l' = l + 1$. This is illustrated in Fig. 1, where we have represented the original potential with $l = 0$, $l = 1$, and $l = 2$ (thick lines) and the SRP potential obtained numerically (dotted line). These numerical results have been obtained on a mesh containing 400 points, ranging from 0 to 20 fm and with a vanishing boundary condition. The thin solid line is the analytical result given by Eq. (45). The slight difference between the thin solid line and the dotted line gives an estimate of the error of the numerical algorithm, which

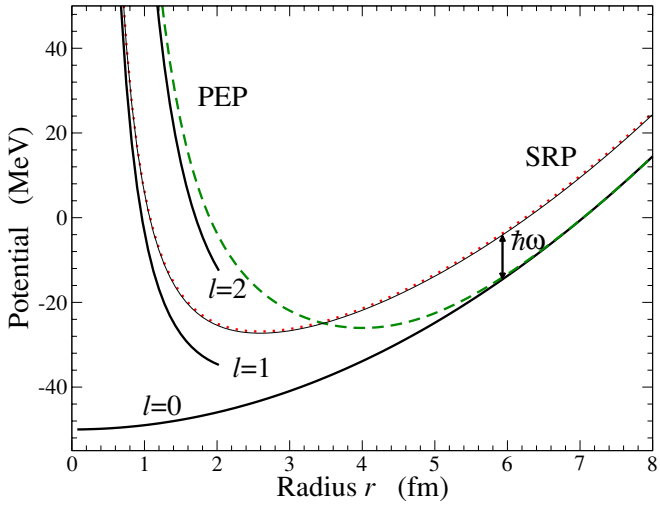

FIG. 1. (Color online) Radial part of the harmonic oscillator potential (H-O) for $l = 0$, 1, and 2 (thick lines) compared with its SRP (dotted line) and PEP (dashed line) transformation of the $l = 0$ potential. The thin solid line stands for $v_{\text{H-O}}(l = 1) + \hbar\omega$.

appears to be very small. This illustrates the shape invariance property [4] of the harmonic oscillator.

Generalizing this result to the removal of several core states we remark that, in the new radial Hilbert space, up to a translation of $n_c\,\hbar\omega$, where n_c is the number of removed core orbitals with angular momentum l, the Pauli principle maps the original potential with angular momentum l to a new potential analogous to the radial potential with an effective angular momentum $l' = l + n_c$. However, only the radial wave function is affected by the effective angular momentum; the angular part of the wave function is unchanged by the SuSy mapping.

As we have already mentioned, this SRP transformation changes the phases. The restoration of the phases is ensured by the PEP transformation. From the analytic expression of $\underline{v}_1^l$ [cf. Eq. (46)], we see that near $r \sim 0$, $\underline{v}_1^l(r) \,\tilde{0}\, v_0^{l+2}(r)$, and asymptotically, $\underline{v}_1^l(r) \approx v_0^l(r)$. The potential $\underline{v}_1^l(r)$ is represented in Fig. 1 (dashed line). The restoration of the phases imposes a nontrivial transformation of the potential: near zero, the potential $\underline{v}_1$ is mapped to a new potential analogous to $v_0^{l'}$ with a centrifugal force analogous to an effective angular momentum $l' = l + 2n_c$, and asymptotically, the potential remains unchanged as required by phase conservation. This behavior is the consequence of the Pauli principle and phase restoration.

The mapping operators $\hat{\mathrm{u}}_0^l$ can also be analytically derived, and we will discuss the properties of these operators from their asymptotic (where all radii go to infinity) expressions:

$$\langle r|\mathrm{u}_0^{l+}|r'\rangle \underset{r,r'\to\infty}{\sim} -\langle r|\frac{1/\sqrt{2}}{\sqrt{\hat{p}^2/2m - E_0^0}}\,(i\hat{q} + \hat{x})\,|r'\rangle, \qquad (47)$$

$$\langle r|\underline{\mathrm{u}}_0^{l\pm}|r'\rangle \underset{r,r'\to\infty}{\sim} \delta(r - r'). \qquad (48)$$

Hence, whereas the operator $\hat{\mathrm{u}}_0^{l\pm}$ is never trivial, even at large distances the operator $\underline{\hat{\mathrm{u}}}_0^{l\pm}$ reduces to the unity operator for large r. This is a consequence of phase restoration. As a result,

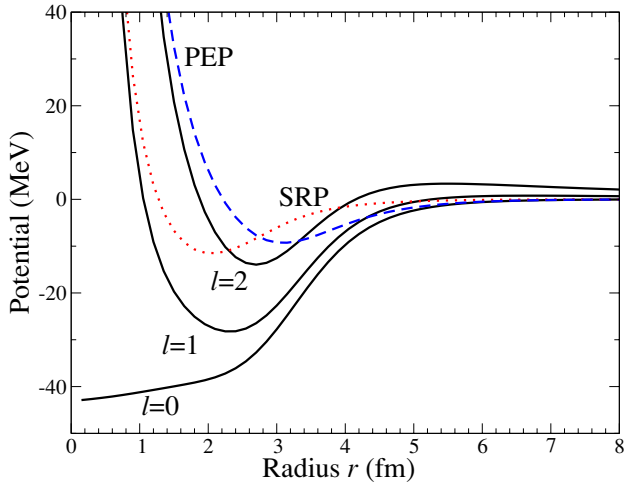

FIG. 2. (Color online) Radial part of the core-halo potentials v_0^l (solid lines) for $l = 0$, 1, and 2 and the SuSy-transformed $v_1^{l=0}$ (dashed line) and $\underline{v}_1^{l=0}$ (dotted line).

the PEP transformations do not modify observables, which are only sensitive to the asymptotic part of the wave functions. These asymptotic properties are also valid for other potentials, as illustrated for halo nuclei potential in the next paragraph.

B. Halo nuclei potentials

The study of the properties of weakly bound systems has received renewed interest after the discovery of halo nuclei [20]. These systems have very large mean-square radii and small separation energies. In fact, the separation energy of the nucleons forming the halo is so small that their degrees of freedom can be separated from those of the nucleon constituents of the core. Up to now, this property has only been observed in light nuclei close to the nucleon drip-lines such as ^{6}He, ^{11}Be, or ^{19}C. In Ref. [21], the proposed core-halo potential for ^{11}Be is the sum of a Wood-Saxon potential and a surface potential

$$v_0^{l=0}(r) = v_0 f(r) + 16a_0^2 a_1 \left(\frac{df(r)}{dr}\right)^2,$$

where $f(r) = [1 + e^{(r-r_0)/a_0}]^{-1}$ is a Wood-Saxon potential and the parameters are $v_0 = -44.1$ MeV, $a_1 = -10.15$ MeV, $r_0 = r_0^1 A^{1/3}$ with $r_0^1 = 1.27$ fm, and $a_0 = 0.75$ fm. The bound states of this potential are $1s$ states at -25.0 and -0.5 MeV and a $1p$ state at -11 MeV. For simplicity we omit the spin-orbit coupling and consider a model case where the $1s$ and $1p$ orbitals are occupied by the core neutrons. Thus, these two orbitals are Pauli blocked and cannot be filled in by the neutron of the halo. In its ground state the latter occupies the $2s$ state.

We work on a constant-step mesh containing 400 points and ranging from 0 to 50 fm. We show in Fig. 2 the original potential v_0^l for $l = 0$, $l = 1$, and $l = 2$ (solid lines), the SRP $v_1^{l=0}$ (dashed line), and the PEP $\underline{v}_1^{l=0}$ (dotted line).

We can obtain analytical expressions near $r = 0$ and for large r. Indeed, near zero, the lowest energy state, with an energy E_0^{0l}, behaves like r^{l+1}; asymptotically, it behaves like

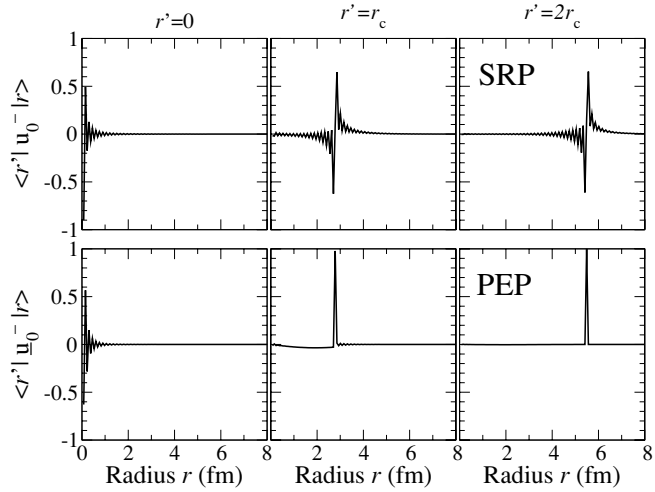

FIG. 3. Matrix elements $\mathrm{u}_0^-(r, r')$ (top, SRP) and $\underline{\mathrm{u}}_0^-(r, r')$ (bottom, PEP) for several values of r' ($r' = 0, r_c, 2r_c$) calculated for the angular momentum $l = 0$ inside the core-halo potential. Recall that r_c is the radius of the ^{10}Be core.

$\exp(-\gamma_0 r)$ with $\gamma_0 = \sqrt{-2m E_0^{0l}}/\hbar$. These asymptotics and therefore the following expressions are very general for all potentials that are regular at the origin and vanish for large r. We find that the superpotentials behave like ($r \to 0$)

$$w_0^l(r) \underset{r\to 0}{\sim} \frac{l+1}{r} \text{ and } w_0^l(r) \underset{r\to\infty}{\sim} -\gamma_0, \tag{49}$$

$$\underline{w}_0^l(r) \underset{r\to 0}{\sim} \frac{2l+3}{r} \text{ and } \underline{w}_0^l(r) \underset{r\to\infty}{\sim} 0, \tag{50}$$

and the potentials for $r \to 0$ are

$$v_1^l(r) \underset{r\to 0}{\sim} v_0^l(r) + \frac{\hbar^2}{m}\frac{l+1}{r^2} = v_0^{l+1}(r), \tag{51}$$

$$\underline{v}_1^l(r) \underset{r\to 0}{\sim} v_0^l(r) + \frac{\hbar^2}{m}\frac{2l+3}{r^2} = v_0^{l+2}(r), \tag{52}$$

and for $r \to \infty$ they are

$$v_1^l(r) \underset{r\to\infty}{\sim} v_0^l(r), \tag{53}$$

$$\underline{v}_1^l(r) \underset{r\to\infty}{\sim} v_0^l(r). \tag{54}$$

The creation/annihilation operators become

$$\hat{a}_0^{\pm} \underset{r\to\infty}{\sim} \mp\frac{i\,\hat{p}}{\sqrt{2m}} - \gamma_0, \tag{55}$$

$$\underline{\hat{a}}_0^{\pm} \underset{r\to\infty}{\sim} \mp\frac{i\,\hat{p}}{\sqrt{2m}} + \gamma_0. \tag{56}$$

Using these asymptotic expressions, one finds the following properties of the mapping operators:

$$\langle r|\hat{\mathrm{u}}_0^{\pm}|r'\rangle \underset{r\to\infty}{\sim} \langle r|\frac{\mp i\,\hat{p}/\sqrt{2m} - \gamma_0}{\sqrt{\hat{p}^2/2m + \gamma_0^2}}|r'\rangle, \tag{57}$$

$$\langle r|\underline{\hat{\mathrm{u}}}_0^{\pm}|r'\rangle \underset{r\to\infty}{\sim} \delta(r - r'). \tag{58}$$

We present in Fig. 3 the matrix elements $\langle r|\hat{\mathrm{u}}_0^-|r'\rangle$ and $\langle r|\underline{\hat{\mathrm{u}}}_0^-|r'\rangle$ as a function of r for several values of r': $0, r_c$, and $2r_c$, where r_c is the radius of the ^{10}Be core. The peaks identify the diagonal terms. We remark that the operator $\hat{\mathrm{u}}_0^-$ has important off-diagonal terms (for small and large values of r') whereas the operator $\underline{\hat{\mathrm{u}}}_0^-$ converges toward a δ function when r' increases. Hence, the restoration of the phase shift imposes $\underline{\hat{\mathrm{u}}}_0^{\pm} \sim \hat{1}$ for large values of r'; however, this relation breaks down close to the core where the off-diagonal terms become important.

V. ELECTRIC EXCITATION

In this section, we shall consider dynamical properties of nuclei within the consistent SuSy transformation we have developed in the previous sections and discuss how they can be approximated. We will discuss the modifications of the excitation operators and the doorway sensitivity will compute some transition elements and strength associated with monopole ($E0$), dipole ($E1$), and quadrupole ($E2$) electromagnetic excitations and the associated sum rules. The potential considered is the Wood-Saxon potential of Sec. IV B.

We assume that, prior to any SuSy transformation, the excitation operator takes the standard multipolar form

$$\hat{f}_0(\lambda, L, M) = \hat{f}_0^{\mathrm{rad}}(\lambda)\hat{Y}_{LM}, \tag{59}$$

with the radial excitation operator $\hat{f}_0^{\mathrm{rad}}(\lambda) = \hat{r}^{\lambda}$. We drop the coupling constant because we are only interested in the transformation of the radial excitation operator and the relative difference between the consistent SuSy transformation and its approximations. The $E0$ transition is induced by $\hat{f}_0(2, 0, 0)$ and the electromagnetic transitions $E\lambda$ are induced by $\hat{f}_0(\lambda, \lambda, M)$ ($\lambda \geqslant 1$). The SuSy transformation of the excitation operator is

$$\hat{f}_{\mathrm{A_c}}(\lambda, L, M) = \hat{\mathrm{U}}_{\mathrm{A_c}}^-\, \hat{f}_0(\lambda, L, M)\, \hat{\mathrm{U}}_{\mathrm{A_c}}^+. \tag{60}$$

By introducing explicitly the angular momentum quantum numbers and assuming that at maximum one level per angular momentum is occupied by the core nucleons, the radial excitation operator between two angular momenta l and l' occupied by the core nucleons in $h = (n = 1, l)$ and $h' = (n' = 1, l')$ is thus given by

$$\hat{f}_{\mathrm{A_c}}^{l'l}(\lambda) = \hat{\mathrm{u}}_0^{l'-}\, \hat{f}_0^{\mathrm{rad}}(\lambda)\, \hat{\mathrm{u}}_0^{l+}, \tag{61}$$

If l' or l is not occupied by a core nucleon the corresponding $\hat{\mathrm{u}}$ should be replaced by the identity. The external operator $\hat{f}_{\mathrm{A_c}}^{l'l}(\lambda)$ allows transitions among different angular momentum spaces according to the selection rules deduced from the relation

$$\langle l'm'|\hat{f}_{\mathrm{A_c}}(\lambda, L, M)|lm\rangle = \hat{f}_{\mathrm{A_c}}^{l'l}(\lambda)\langle l'm'|\hat{Y}_{LM}|lm\rangle. \tag{62}$$

It should be noticed that in Eq. (61) the mapping operators $\hat{\mathrm{u}}_0^{l\pm}$ on the right and left sides of $\hat{f}_0^{\mathrm{rad}}(\lambda)$ may not correspond to the same angular momentum l. Moreover, whereas the original radial excitation operator $\hat{f}_0^{\mathrm{rad}}(\lambda)$ is diagonal (in the coordinate space), $\hat{f}_{\mathrm{A_c}}^{l'l}(\lambda)$ is no longer diagonal because the transformation operators $\hat{\mathrm{u}}_0^{l\pm}$ are nonlocal.

A. Consistent excitation operator and its approximations

In the following, we shall calculate the excitation operator and some of the observables it induces. In the literature, the

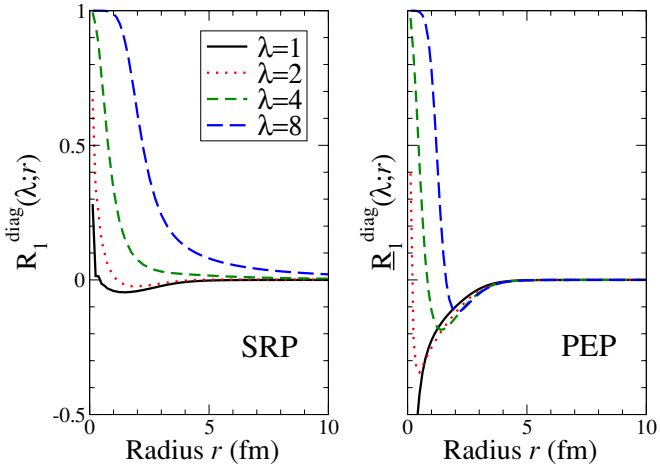

FIG. 4. (Color online) The normalized difference of diagonal matrix elements $[R_1^{\rm diag}(\lambda;r)$ for the SRP transformation and $\underline{R}_1^{\rm diag}(\lambda;r)$ for the PEP one] represented for several values of λ (1, 2, 4, and 8) for the electric excitation $E\lambda$ inside the s subspace.

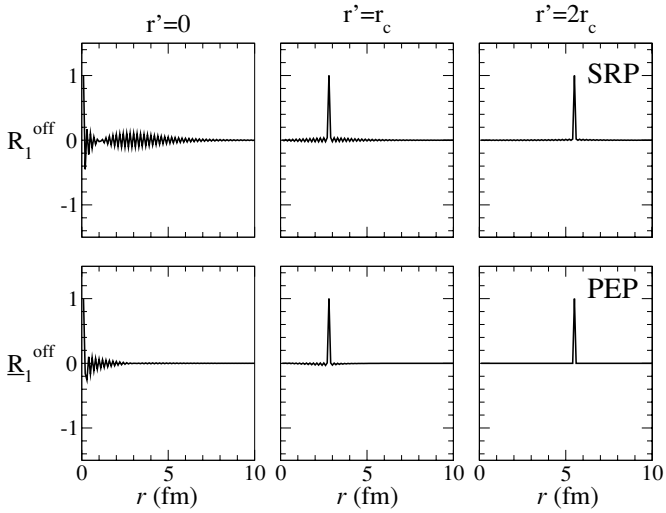

FIG. 5. The normalized off-diagonal matrix elements $[R_1^{\rm off}(\lambda=4;r,r')$ and $\underline{R}_1^{\rm off}(\lambda=4;r,r')]$ represented as a function of r for several values of r' $(0, r_c, 2r_c)$ for the electric excitation $E\lambda$ inside s subspace.

SuSy transformation is in general not applied to the excitation operator. Hence, instead of calculating the matrix elements induced by the consistent excitation operator $\hat{f}^{l'l}_{\rm A_c}(\lambda)$, the authors have evaluated the matrix elements of $\hat{f}^{\rm rad}_0(\lambda)$ with the SuSy-transformed wave functions. We will refer to this approximation as the *internal* approximation. We introduce a second approximation called the *diagonal* approximation that consists simply of neglecting the off-diagonal terms in coordinate space of the consistent excitation operator.

As a first example we will study the $E0$ excitation of the halo neutron in the s subspace. In this subspace the core blocks one orbital ($1s$) so that we have to perform an SRP or a PEP transformation to remove this occupied state from the halo Hilbert space and restore the phase shift. Of course, to be complete we also have to remove the occupied p state but since the SuSy transformation is block diagonal for the angular momentum quantum numbers this does not modify the dynamics in the s subspace.

To evaluate the difference between the consistent SuSy transformation and its approximations, we define two quantities

$$R^{\rm diag}_{\rm A_c}(\lambda;r)=\frac{\langle r|\Delta\hat{f}^{00}_{\rm A_c}(\lambda)|r\rangle}{\langle r|\hat{f}^{00}_{\rm A_c}(\lambda)|r\rangle}, \tag{63}$$

$$R^{\rm off}_{\rm A_c}(\lambda;r,r')=\frac{\langle r|\hat{f}^{00}_{\rm A_c}(\lambda)|r'\rangle}{\langle r|\hat{f}^{00}_{\rm A_c}(\lambda)|r\rangle}, \tag{64}$$

where

$$\Delta\hat{f}^{l'l}_{\rm A_c}(\lambda)=\hat{f}^{l'l}_{\rm A_c}(\lambda)-\hat{f}^{\rm rad}_0(\lambda) \tag{65}$$

is the difference between the excitation operator consistently transformed $\hat{f}^{l'l}_{\rm A_c}(\lambda)$ and the original excitation operator $\hat{f}^{\rm rad}_0(\lambda)$. The ratio $R^{\rm diag}_{\rm A_c}(\lambda;r)$ evaluates the difference between the diagonal part of the consistent excitation operator and the original operator, normalized to the value of the diagonal part of the consistent operator. It gives an evaluation of the approximation for the diagonal part of the excitation operator. Figure 4 shows the ratio $R^{\rm diag}_{\rm A_c}(\lambda;r)$ and $\underline{R}^{\rm diag}_{\rm A_c}(\lambda;r)$ for $\lambda=1,2,4$, and for 8 the $1s$ SRP and PEP transformations, respectively. We remark that, for large radii r, the diagonal part of the excitation operator is close to the original one $[R^{\rm diag}_{\rm A_c}(\lambda;r)\sim 0]$. This is a consequence of the asymptotic properties of the mapping operator as has been discussed in Sec. IV B. For small radii r, the diagonal part of the excitation operator is strongly modified, with the ratio $R^{\rm diag}_{\rm A_c}(\lambda;r)\sim 1$ revealing that $\langle r|\hat{f}^{\rm rad}_{\rm A_c}|r\rangle \gg \langle r|\hat{f}^{\rm rad}_0|r\rangle$. This difference persists through a large range of radial coordinates. This range increases with λ and is wider for SRP transformations compared with PEP transformations.

In contrast, the ratio $R^{\rm off}_{\rm A_c}(\lambda;r,r')$ evaluates the amplitude of the off-diagonal terms in coordinate space normalized to the diagonal term of the consistent excitation operator. In Fig. 5, we represent the ratio $R^{\rm off}_{\rm A_c}(\lambda=4;r,r')$ and $\underline{R}^{\rm off}_{\rm A_c}(\lambda=4;r,r')$ for the SRP and PEP transformations, respectively, and for three values of r': 0, r_c, and $2r_c$. For the SRP transformation, off-diagonal terms are important for small r' and decrease in relative magnitude while r' increases. Off-diagonal terms are nonzero over a wide range and we will show in the next paragraphs that they can have a more important effect on observables than the diagonal terms. For the PEP transformation the off-diagonal terms are smaller and become negligible for intermediate and large r' ($\geqslant r_c$), as required by the restoration of asymptotic behavior.

In all the cases presented here, the consistent excitation operator is different from the original one in the space region inside the core potential. Hence, from this observation, we can expect that there will be important effects induced by the consistent calculation if and only if the calculated observable is sensitive to the space region inside the core potential.

B. Transformation of the doorway state

We want now to evaluate contributions of both the diagonal and the off-diagonal excitation operators to the matrix

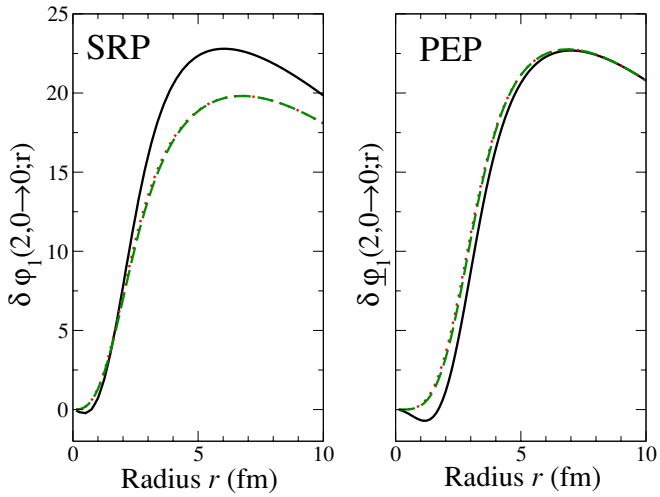

FIG. 6. (Color online) The doorway state $\delta\varphi_1(\lambda = 2, 0 \to 0; r)$ and $\delta\underline{\varphi}_1(\lambda = 2, 0 \to 0; r)$ of electric excitations for the SRP and the PEP transformations, respectively. The solid line stands for the consistent excitation operator, the dotted line for the internal approximation, and the dashed line for the diagonal approximation.

elements. For that, we introduce the doorway state defined as

$$|\delta\varphi_{\mathrm{A_c}}(\lambda, l \to l')\rangle = \hat{f}^{l'l}_{\mathrm{A_c}}(\lambda)\big|\varphi^{l}_{\mathrm{A_c}}\big\rangle,$$

which shows the effect of the excitation considered on the wave functions, particurly, the contribution of the off-diagonal elements. In the following, we have chosen for $|\varphi^{l}_{\mathrm{A_c}}\rangle$ the ground state of $\hat{h}^{l}_{\mathrm{A_c}}$.

We represent in Fig. 6 the doorway state $\delta\varphi_1(\lambda = 2, 0 \to 0; r)$ and $\delta\underline{\varphi}_1(\lambda = 2, 0 \to 0; r)$ for the SRP and PEP transformations, respectively. The solid line stands for the consistent excitation operator, the dotted line for the *internal* approximation, and the dashed line for the *diagonal* approximation. We remark that the *internal* approximation and the *diagonal* approximation are indistinguishable. This shows that off-diagonal terms are the most important sources of modification of the excitation operator.

Moreover, the consistent doorway state changes sign whereas the two approximations remain positive. This affects the node structure of the wave function and may induce strong modifications for forbidden transition as we will see in the next paragraph.

We use the doorway state to evaluate the mean radius of the halo. For the $2s$ state, it is defined as

$$\langle r^2\rangle_{\mathrm{A_c}} = \big\langle\varphi^{2s}_{\mathrm{A_c}}\big|\hat{f}^{00}_{\mathrm{A_c}}(2)\big|\varphi^{2s}_{\mathrm{A_c}}\big\rangle. \tag{66}$$

Using a 400-point mesh going up to 60 fm, we find that $\langle r^2\rangle_0 = \langle r^2\rangle_1 = \langle \underline{r}^2\rangle_1 = 7.21 \pm 0.03$ fm, and for the internal approximations $\langle \tilde{r}^2\rangle_1 = 6.48$ fm and $\langle \underline{\tilde{r}}^2\rangle_1 = 7.27$ fm with the same precision. As expected (cf. Fig. 6), the internal SRP approximation underestimates the mean radius and the internal PEP approximation slightly overestimates the mean radius. The maximum value of the integrand involved in the calculation of the mean radius is around 20 fm. At this distance of the core, the internal approximation of the PEP transformation is very good, and the SRP transformation is still rather good. In the following we will show that the internal approximation of the SuSy transformation is rather good for peripheral observables or for the excitation field, as in the case of the mean radius of a one-neutron halo. But we expect more important effects in the case of two neutrons interacting in the halo because the neutron-neutron interaction occurs inside the core potential.

TABLE I. $\underline{B}_1(E0, 2s \to ns)$ for the PEP transformed harmonic oscillator potential. $\underline{\widetilde{B}}_1(E0, 2s \to ns)$ is the matrix element induced by the *internal* approximation of the excitation operator.

$\underline{f}$	$3s$	$4s$	$5s$	$6s$	$7s$
$\underline{B}_1(E0)$	1.1×10^4	$o(10^{-4})$	$o(10^{-8})$	$o(10^{-7})$	$o(10^{-7})$
$\underline{\widetilde{B}}_1(E0)$	9.2×10^3	1.5×10^1	1.3	7.1×10^{-2}	1.4×10^{-4}

C. Single-particle reduced transition probability

The single-particle reduced transition probabilities are defined as [22]

$$B_{\mathrm{A_c}}(E0, i \to f) = \big\langle\varphi^{f}_{\mathrm{A_c}}\big|\hat{f}^{l_f l_i}_{\mathrm{A_c}}(2)\big|\varphi^{i}_{\mathrm{A_c}}\big\rangle \tag{67}$$

with $l_f = l_i$ and as

$$B_{\mathrm{A_c}}(E\lambda, i \to f) = \big\langle\varphi^{f}_{\mathrm{A_c}}\big|\hat{f}^{l_f l_i}_{\mathrm{A_c}}(\lambda)\big|\varphi^{i}_{\mathrm{A_c}}\big\rangle \tag{68}$$

with $|l_i - \lambda| \leqslant l_f \leqslant l_i + \lambda$ and for $\lambda \geqslant 1$. To simplify the notation, the states i and j are labeled according to the original space prior to any transformation. In the halo case, as developed here, all the final states are in the continuum so it will not be possible to use directly these definitions. In the next section we will introduce the strength function, a more general way to look at transition probabilities that is suitable for the case of excitation toward the continuum and that can thus be used in the halo case. To get results for the transition probabilities between discrete states, in the present section, we will restrict the discussion to the harmonic oscillator model (see Sec. IVA). To simplify the discussion, we will consider that the nucleons of the core only occupy the $1s$ orbital and we will study the excitation of an additional neutron in the $2s$ orbital. We have computed numerically the reduced matrix elements $\underline{B}_1(E0)$ and $\underline{B}_1(E1)$ for the PEP transformation. The results are presented, respectively, in Tables I and II. In the harmonic oscillator, because of selection rules, from the $2s$ state the monopole operator $\hat{r}^2$ can induce transition only toward the $3s$ state. In Table I, the first line shows the result of the matrix elements (B) induced by the consistent excitation

TABLE II. $\underline{B}_1(E1, 2s \to np)$ for the PEP transformed harmonic oscillator potential. $\underline{\widetilde{B}}_1(E1, 2s \to np)$ is the matrix element induced by the *internal* approximation of the excitation operator.

$\underline{f}$	$1p$	$2p$	$3p$	$4p$	$5p$
$\underline{B}_1(E1)$	5.0×10^2	1.2×10^3	$o(10^{-6})$	$o(10^{-7})$	$o(10^{-6})$
$\underline{\widetilde{B}}_1(E1)$	1.2×10^3	8.0×10^2	9.5	1.2	7.8×10^{-2}

operator. As expected, the forbidden transition are zero within the numerical uncertainty indicated in parenthesis.

The matrix elements $\widetilde{B}$ induced by the *internal* excitation operator are shown in the second line of Table I. For allowed transitions, the *internal* approximation modifies the exact matrix element by about 20%, but the main effect of this approximation is that it induces forbidden transitions from $2s$ to $4s-7s$ states.

However, in the case of the $E1$ electromagnetic transition, the selection rules of dipole transitions in the harmonic oscillator allow transition from $2s$ states to $1p$ and $2p$ states. The same phenomenon is observed in Tables I and II: the *internal* approximation produces spurious excitation of forbidden transitions.

D. Strength

The very important discrepancy between the internal and the complete SuSy observed in the case of the harmonic oscillator might be a peculiarity due to the symmetry of this model. Let us thus return to the physical case of the ^{11}Be halo nuclei for which transitions between orbitals belonging to the same l-space are all allowed. Now we should remove the $1s$ (-25-MeV) and $1p$ (-12-MeV) orbitals occupied by the core neutrons so that only one bound state ($2s$) is available for the halo neutron. The excitations can only promote the halo neutron to the continuum. Hereafter, the eigenstates and the continuum states will be obtained from the diagonalization of the Hamiltonian inside a box going up to 50 fm with 400 points.

To discuss transition toward the continuum, we introduce the strength

$$S_{\mathrm{A_c}}(E\lambda, i, \omega) = \sum_f \left| B_{\mathrm{A_c}}(E\lambda, i \to f) \right|^2 \delta(\omega - E_f + E_i), \quad (69)$$

where i is the initial state, here the $2s$ orbital, and the final states f are the continuum states of the box. The single-particle energies are E_i and E_f, respectively. Since we perform the calculation in a box the continuum is discretized. To obtain a smooth strength function one often smoothes the obtained results with a Gaussian or a Lorentzian function. In this paper we will do both.

Strengths for PEP transformations for $E0$, $E1$, and $E2$ transitions are presented in parts (a) of Figs. 7–9 with a Lorentzian smoothing ($\Gamma = 500$ keV) and in Fig. 10 with a Gaussian smoothing. Part (b) of each figure gives directly the ratio $\underline{B}_1(E\lambda)/\underline{\widetilde{B}}_1(E\lambda)$ computed for individual states.

For the monopole mode, using a Lorentzian smoothing the consistent strength and the internal strength appears to be very similar [see Fig. 7(a)], even if the ratio $\underline{B}_1(E0)/\underline{\widetilde{B}}_1(E0)$ computed for individual states [see Fig. 7(b)] is very different from 1 for large values of the final excitation energy E_f.

The dipole excitations connect the states of two different l-subspaces. On the smoothed $\underline{S}_1(E1)$ strength [see Fig. 8(a)], we observe only a small overestimation of the strength for large values of E_f but again the effect seems much larger on the ratio $\underline{B}_1(E1)/\underline{\widetilde{B}}_1(E1)$. In Fig. 9, we represent the strength $\underline{S}_1(E2)$. In the $l = 2$ subspace, there are no core states

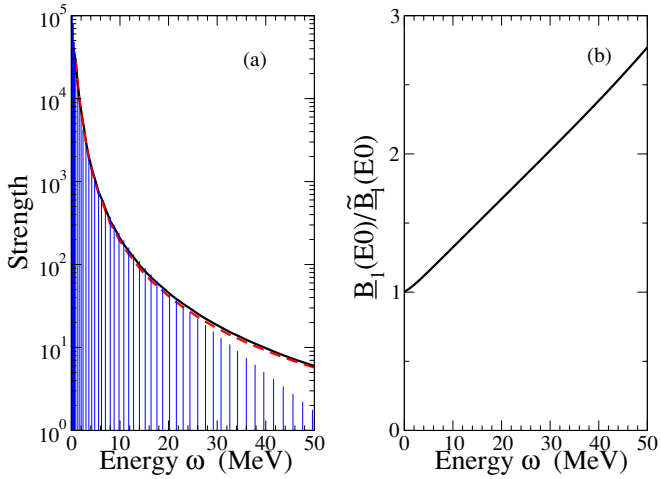

FIG. 7. (Color online) Monopole excitation. (a) The bars are the reduced transition probabilities $\underline{B}_1(E0)$ for the continuum states discretized in the considered box, the solid line is the strength function resulting from a Lorentzian smoothing ($\Gamma = 500$ keV), and the dashed line is the result of the *internal* approximation. (b) The ratio $\underline{B}_1(E0)/\underline{\widetilde{B}}_1(E0)$.

and, consequently, the SuSy transformation is in fact unity. The smoothed strength appears to be only slightly underestimated by the internal approximation, again in contradiction with the ratio $\underline{B}_1(E2)/\underline{\widetilde{B}}_1(E2)$, which exhibits a strong discrepancy.

To solve the contradiction we have first studied the role of the smoothing. We have found that the situation is different with a Gaussian smoothing, as illustrated in Fig. 10. This difference is due to the difference in the tails of the two smoothing functions: The long tails of the Lorentzian function associated with the low-energy states, which have a large $\underline{B}_1(E0)$, dominate even at large energy when a Lorentzian form factor is used. Indeed, since the difference between the two calculations is small for these dominating states the final Lorentzian-smoothed strengths for the two calculations are rather close, in contradiction with the direct ratio of

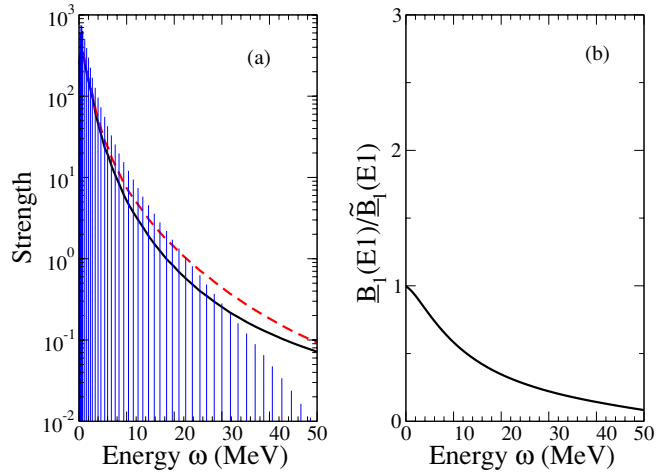

FIG. 8. (Color online) Same as Fig. 7 except for dipole transitions.

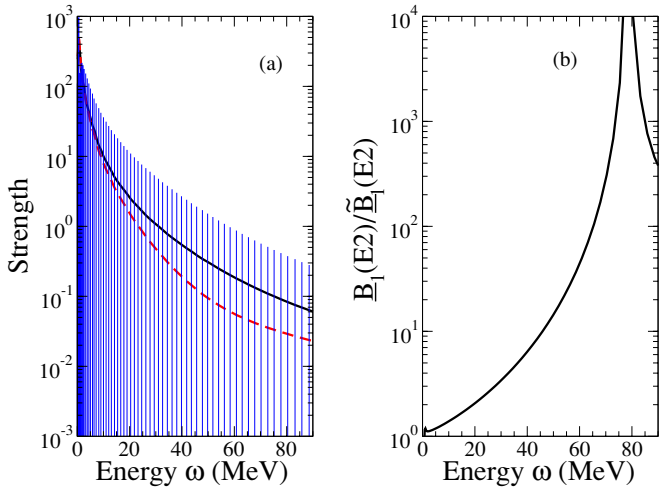

FIG. 9. (Color online) Same as Fig. 7 except for quadrupole transitions.

individual excitation probabilities or the results of the Gaussian smoothing.

To avoid the ambiguity of the smoothing method we have studied the continuum limit by a direct scaling of the numerical box size (we have also tested the role of mesh size). We have observed that the ratio $\underline{B}_1/\widetilde{\underline{B}}_1$ computed for each individual state does not change shape going to the continuum limit whereas the smoothed strengths vary and exhibit a strong dependence on the smoothing functional and parameters. Therefore, the ratio $\underline{B}_1(E0)/\widetilde{\underline{B}}_1(E0)$ provides in fact the correct continuum limit and the large observed discrepancy at high energy between the internal and the complete SuSy transformation is the physical one. This is even better illustrated by considering integrated effects like effects on the sum rules.

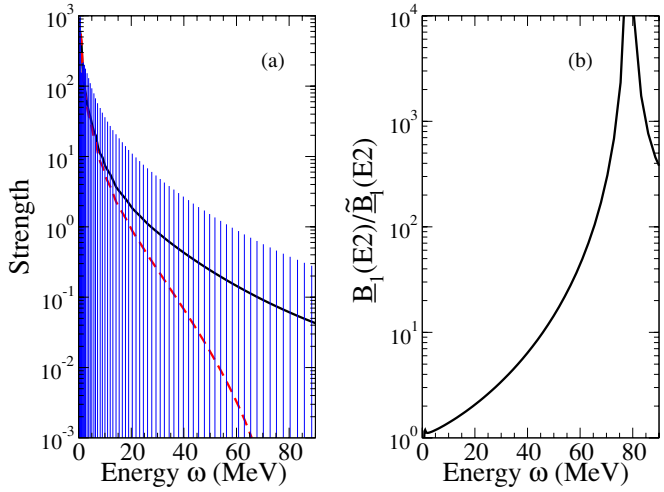

FIG. 10. (Color online) Same as Fig. 9 except with Gaussian smoothing.

TABLE III. Relative error induced in the calculation of the energy-weighted sum rules by the *internal* approximation of PEP transformations.

	$(\underline{m}_0 - \widetilde{\underline{m}}_0)/\underline{m}_0$	$(\underline{m}_1 - \widetilde{\underline{m}}_1)/\underline{m}_1$	$(\underline{m}_2 - \widetilde{\underline{m}}_2)/\underline{m}_2$
$E0$	1.4%	3.9%	17.4%
$E1$	−6.8%	−33.3%	−93.1%

E. Sum rules

By integrating the strength over the energy, we can define different sum rules

$$m_t(E\lambda) \equiv \int d\omega\ \omega^t S(E\lambda, i=0, \omega), \tag{70}$$

where t is the weight of the energy. In the frozen-core approximation, the sum rules m_0 and m_1 can be obtained from the halo wave function according to

$$m_0 = \langle \Phi_v | \hat{f}_0 \hat{\mathrm{P}}_v \hat{f}_0 | \Phi_v \rangle - (\langle \Phi_v | \hat{f}_0 | \Phi_v \rangle)^2, \tag{71}$$

$$m_1 = \tfrac{1}{2} \langle \Phi_v | \big[\hat{f}_0 \hat{\mathrm{P}}_v, \big[\hat{h}_0^l \hat{\mathrm{P}}_v, \hat{f}_0 \hat{\mathrm{P}}_v \big] \big] | \Phi_v \rangle, \tag{72}$$

where $\hat{f}_0$ is the excitation operator defined by Eq. (59). Equations (71) and (72) are the standard sum rules [23] rewritten for projected operators. We define the *internal* approximation for the sum rule as $\widetilde{m}_t$ for which the projector P_v has been removed. The Pauli principle no longer holds. To estimate the error induced in the calculation of $\widetilde{m}_t$ compared to m_t, we have estimated the ratios $(m_t - \widetilde{m}_t)/m_t$, and the results are presented in Table III. The relative error induced by the internal approximation increases with weight. This result is compatible with the results presented in Figs. 7 and 8: When the weight increases, the contribution of large energy increases as do the discrepancies between the consistent SuSy and its internal approximation.

VI. RESPONSE TO A GAUSSIAN EXCITATION

In the previous section, we have shown that the PEP transformation modifies essentially the external excitation operator in the space region located inside the core potential. The electric operators $\hat{r}^\lambda \hat{Y}_{LM}$ studied in the previous section, which can be seen as a multiple expansion of a Coulomb field far from the nucleus or as the low momentum transfer limit of a plane wave scattering, are strong far from the nucleus. Hence, the effect of the PEP transformation on the excitation process has been found not to be too large. However, this is not always the case and, in particular, nuclear scattering and/or large momentum transfer reactions correspond to much shorter distances. To study the effect of the PEP transformation on this kind of scattering, in this section, we study the response to a Gaussian excitation that can strongly overlap the core potential (Wood-Saxon potential of Sec. IV B). A Gaussian potential can be induced by an external nuclear potential as well as a residual two-body interaction between particles in the halo. In a spirit similar to that of the previous section, we will not study a specific process; rather, we will investigate the response to a

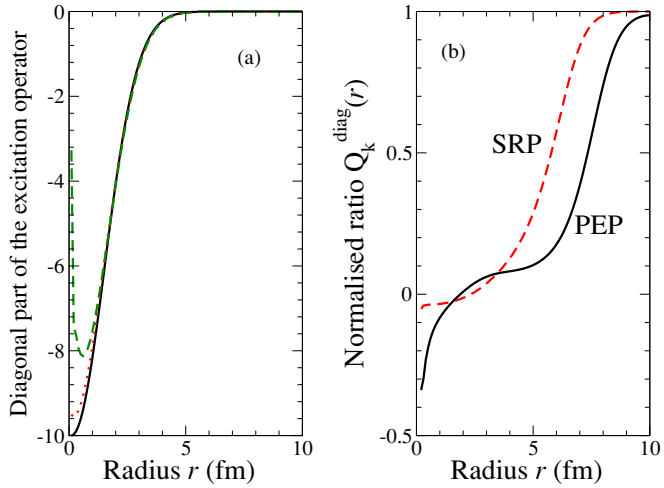

FIG. 11. (Color online) (a) The initial Gaussian potential ($l = 0$) (solid line) and SRP (dotted line) and PEP (dashed line) potentials. (b) The ratio $Q^{\rm diag}_{\rm A_c}(r)$ for SRP (dashed) and PEP (dotted) potentials.

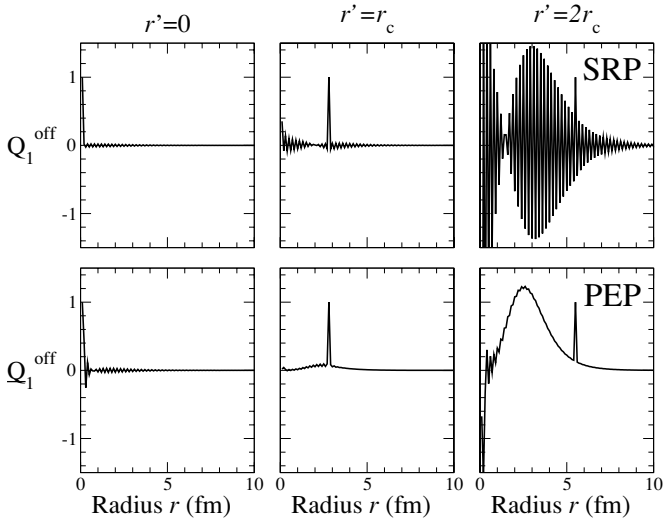

FIG. 12. The ratios $Q^{\rm off}_{\rm A_c}(r, r')$ in the $l = 0$ channel as a function of r for several values of r' (0, r_c, and $2r_c$) in the case of a Gaussian potential.

one-body Gaussian potential centered around $\mathbf{r}_0$ defined as

$$g_0(\mathbf{r}) = -\frac{g_0}{(\sqrt{\pi}\mu)^3}\exp\left(-\frac{(\mathbf{r}-\mathbf{r}_0)^2}{\mu^2}\right),$$

where the norm of the interaction is $g_0 = 450$ MeV $\cdot$ fm^3 and its range is $\mu = 2$ fm. For simplicity, in the present schematic calculation we will assume $\mathbf{r}_0 = 0$. The SuSy transformation of this potential is

$$\hat{g}^{ll}_{\rm A_c} = \hat{\rm u}^{l-}_0 \hat{g}_0 \hat{\rm u}^{l+}_0.$$

Similarly to the previous section, we define two quantities that measure the modification of the SuSy transformation on the diagonal and off-diagonal terms of the Gaussian potential:

$$Q^{\rm diag}_{\rm A_c}(r) = \frac{\langle r|\hat{g}^{00}_{\rm A_c} - \hat{g}^{00}_0|r\rangle}{\langle r|\hat{g}_{\rm A_c}|r\rangle}, \tag{73}$$

$$Q^{\rm off}_{\rm A_c}(r, r') = \frac{\langle r|\hat{g}^{00}_{\rm A_c}|r'\rangle}{\langle r|\hat{g}^{00}_{\rm A_c}|r\rangle}. \tag{74}$$

In Fig. 11, we fix $r_0 = 0$ and we represent (a) the diagonal part of $g_{\rm A_c}$ (dotted line) and $\underline{g}_{\rm A_c}$ (dashed line) compared to the original potential g_0 (solid line) and (b) the ratio $Q^{\rm diag}_{\rm A_c}(r)$ for the SRP transformation (dashed line) and PEP transformation (solid line). In the very central region, the PEP transformations modify the potential by about 30%. At large distance r, because of the Gaussian shape centered on zero of $g_0(r')$, an important relative weight is given to small radii in the summation $\langle r|\hat{g}_{\rm A_c}|r\rangle = \int dr'\langle r|\hat{\rm u}^-|r'\rangle g_0(r')\langle r'|\hat{\rm u}|r\rangle$. The result of this effect is that the range of $\langle r|\hat{g}_{\rm A_c}|r\rangle$ is slightly increased compared to $g_0(r')$ and because of the exponential behavior of the excitation operator this is enough to make the ratio $Q^{\rm diag}_{\rm A_c}(r) \sim 1$.

In Fig. 12, we show the ratio $Q^{\rm off}_{\rm A_c}(r, r')$ for the SRP transformation (upper panel) and the PEP transformation (lower panel) for three different values of r': 0, r_c, and $2r_c$. For values of r' inside the potential, off-diagonal terms are small compared to the diagonal term but they are spread over a large range of coordinates, and their integrated effect can counterbalance their small values. Outside the potential, the off-diagonal terms become very important and even larger than the diagonal term for both SRP and PEP transformations.

Both diagonal and off-diagonal terms have an effect on the particle wave function, which can be estimated with the doorway state

$$\left|\delta\varphi_{\rm A_c}(l \to l)\right\rangle = \hat{g}^{ll}_{\rm A_c}\left|\varphi^l_{\rm A_c}\right\rangle.$$

In the following, we have chosen for $|\varphi^l_{\rm A_c}\rangle$ the ground state of $\hat{h}^l_{\rm A_c}$.

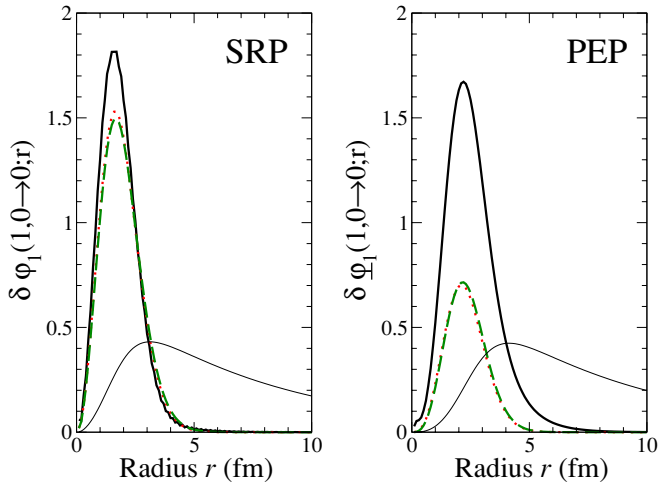

FIG. 13. (Color online) The doorway state in the $l = 0$ channel $\delta\varphi_1(0 \to 0; r)$ produced by a Gaussian excitation for SRP and PEP transformations. The solid line stands for the consistent excitation operator, the dotted line for the internal approximation, and the dashed line for the diagonal approximation. The thin line stands for the initial wave function $\varphi^0_1(r)$.

In Fig. 13, we represent $\delta\varphi_{A_c}(0 \to 0; r)$ for SRP and PEP transformations. The solid line stands for the consistent transformation of the Gaussian interaction, the dotted line for its *internal* approximation, and the dashed line for the *diagonal* approximation. The *internal* approximation and the *diagonal* approximation give about the same results but are both very different from the consistent calculation. These two figures illustrate the importance of the off-diagonal terms, which induce very different doorway states.

Summarizing our results, we can assert that the Gaussian interaction is considerably modified by the SuSy transformations and the *internal* approximation is certainly a bad approximation, as is illustrated in Fig. 13. Hence, calculations of structure properties and reaction mechanism that involve SuSy transformations should never neglect the transformation of the excitation operator (or residual interaction) for radii inside the core potential.

VII. CONCLUSION

In this article, we discussed a consistent framework to perform a quantum mechanics SuSy transformation to take into account the internal degrees of freedom in a core approximation. This method is totally equivalent to the full projector method and is formally very interesting since it provides justifications for effective core-nucleon interactions and nucleon-nucleon residual interaction. In this study, we have considered several kinds of external fields and performed a consistent SuSy transformation. The consistent SuSy transformation provides equivalent effective interactions between composite particle systems and thus can be safely used to describe nuclear structure and reaction of nuclei. The consistent transformation of additional fields as well as the transformation of the wave functions (or the observables) is usually neglected in the literature (internal approximation) and we have shown that such neglect is not always justified.

Our conclusions are the following: For electromagnetic-induced transitions, a consistent SuSy transformation conserves all selection rules whereas the *internal* approximation violates it. Performing different comparisons we have shown that the discrepancies might be large, affecting the node structure of the doorway states and changing the transition probabilities by sizeable factors. Even the sum rules can be affected by a large percentage, (e.g., 33% for the energy-weighted sum rule of the dipole excitation). Hence, the use of the *internal* approximation for the external excitation operator might be dangerous and the results obtained should be carefully discussed. However, the main discrepancies between the consistent calculation and its *internal* approximation appear for external fields, which strongly overlap the core potential. For instance, such is the case of the Gaussian interaction centered at small distance ($r_0 < r_c$).

We have shown that with the SuSy transformation the off-diagonal terms of the external fields are often more important than the diagonal ones. This forbids an approximation that would take into account only the SuSy modification of the diagonal term. Hence, the SuSy transformation has to be fully implemented to preserve the symmetry of the original Hamiltonian.

The entire discussion related to the excitation operator is valid for the observables. Since the wave functions are transformed either they should be transformed back before evaluating average values or the observables should be also transformed before being applied on a transformed state.

In conclusion, in this article, we have stressed the importance of maintaining a consistent quantum mechanics SuSy framework when there is an overlap between the core potential and the additional interactions (excitation operator or observables). For instance, in a recent article Hesse *et al*. [9] have performed the *internal* SuSy approximation and they have shown that, to reproduce the known binding energies and radii of ^{6}He, ^{11}Li, and ^{14}Be halo nuclei, a readjustment of the core-neutron interaction is required. This effect might be induced by the *internal* SuSy approximation, which treats improperly the r^2 observable for the halo neutrons and the residual interaction between them. The consistent SuSy framework would be a way to extract information concerning neutron-neutron interaction in the halo because there is a unique mapping between the original known interaction and the effective one, which includes consistent removal of core orbits.

ACKNOWLEDGMENTS

We are grateful to Daniel Baye, Armen Sedrakian, and Piet Van Isacker for helpful comments on the first version of this paper.

[1] E. Witten, Nucl. Phys. **B188**, 513 (1981).
[2] A. A. Andrianov, N. V. Borisov, and M. V. Ioffe, Phys. Lett. **A105**, 19 (1984).
[3] C. V. Sukumar, J. Phys. A **18**, 2917 (1985).
[4] D. Baye, Phys. Rev. Lett. **58**, 2738 (1987).
[5] F. Cooper, A. Khare, and U. Sukhatme, Phys. Rep. **251**, 277 (1995).
[6] D. Ridikas *et al*., Nucl. Phys. **A609**, 21 (1996).
[7] P. Capel *et al*., Phys. Lett. **B552**, 145 (2003).
[8] B. Gönül *et al*., Eur. Phys. J. A **9**, 19 (2000).
[9] M. Hesse *et al*., Phys. Lett. **B455**, 1 (1999).
[10] I. J. Thompson *et al*., Phys. Rev. C **61**, 24318 (2000).
[11] F. Cannata and M. Ioffe, J. Phys. A **34**, 1129 (2001).
[12] P. Descouvemont, C. Daniel, and D. Baye, Phys. Rev. C **67**, 44309 (2003).
[13] H. Leeb, S. A. Sofianos, J. M. Sparenberg, and D. Baye, Phys. Rev. C **62**, 64003 (2000).
[14] A. M. Shirokov and V. N. Sidorenko, Phys. Atom. Nucl. **63**, 1993 (2000); Yad. Fiz. **63**, 2085 (2000).

[15] B. F. Samsonov and F. Stancu, Phys. Rev. C **67**, 054005 (2003).
[16] K. Chadan and P. C. Sabatier, *Inverse Problems in Quantum Scattering Theory* (Springer-Verlag, Berlin, 1977).
[17] D. Baye, J. Phys. A **20**, 5529 (1987).
[18] L. U. Ancarani and D. Baye, Phys. Rev. A **46**, 206 (1992).
[19] R. D. Lawson, *Theory of the Nuclear Shell Model* (Clarendon Press, Oxford, 1980).
[20] I. Tanihata *et al*., Phys. Rev. Lett. **55**, 2676 (1985).
[21] S. Grévy, O. Sorlin, and N. Vinh Mau, Phys. Rev. C **56**, 2885 (1997).
[22] A. Bohr and B. Mottelson, *Nuclear Structure* (Benjamin, Reading, 1969), Vols. 1 and 2.
[23] P. Ring and P. Schuck, *The Nuclear Many-Body Problem* (Springer-Verlag, Berlin/Vienna/New York, 1980).